SHORT BUNCHES AT THE TRANSITION FROM STRONG TO WEAK LONGITUDINAL INSTABILITY*

Peter Kuske[1], Helmholtz-Zentrum Berlin für Materialien und Energie GmbH, Berlin, Germany and Humboldt-Innovation GmbH, Berlin, Germany

Abstract

The interaction of particles with their vacuum surroundings can lead to longitudinal instabilities of the whole bunch of particles. Most of these instabilities are strong and the growth rates are large compared to the damping rate. For a weak instability the opposite is true and with just a resistive impedance the instability would always be weak and independent of the bunch length. The interaction of a bunch with its own radiation emitted midway between parallel plates leads to a strong instability for long bunches and a transition to weak instability if the bunch length becomes shorter. This regime is analysed numerically with a Vlasov-Fokker-Planck solver. The results are compared to recent observations at ANKA. An attempt is made to explain the remaining discrepancies by including higher order terms of the momentum compaction factor into these calculations. There are indications that the simple model needs refinements in order to take radiation from upstream dipoles into account.

INTRODUCTION

Recently new results from the storage ring ANKA on the longitudinal instability threshold of short bunches were published [1] which show the earlier predicted feature of a stable region above a lower lying threshold which was attributed to a weak instability [2]. These predictions were based on the simple model of bunches circulating between perfectly conducting plates and the interaction of these bunches with their own field emitted on the circular path. The transition from the strong to the weak longitudinal instability occurs as the bunch length becomes shorter. In this paper the transition is studied theoretically in more detail and results of simulations for the actual conditions of the experiments at ANKA will be compared with the observations.

BASIS OF THE SIMULATIONS

The Vlasov-Fokker-Planck (VFP) equation describes the temporal evolution of an ensemble of electrons by their smooth distribution function, $\psi(q,p,\tau)$, written in terms of the normalized phase-space coordinates: $q=z/\sigma_z$, $p=(E_0-E)/\sigma_E$, and τ, in units of the synchrotron period, $1/\omega_s$. The low current rms bunch length, σ_z, and the natural energy spread, σ_E, are related by: $\omega_s\sigma_z/c=\alpha\sigma_E/E_0$ with c, the speed of light, and α, the momentum compaction factor. The evolution of the distribution depends on the radiation excitation and damping, and the interaction of the particles [3]:

$$\frac{\partial\psi}{\partial\tau}+p\frac{\partial\psi}{\partial q}-\left[q+F_c(q,\tau,\psi)\right]\frac{\partial\psi}{\partial p}=2\beta\frac{\partial}{\partial p}\left(p\psi+\frac{\partial\psi}{\partial p}\right)$$

The r.h.s. is the Fokker-Planck-term introduces damping and diffusion due to synchrotron radiation with $ß=1/\omega_s\tau_d$, the longitudinal damping time, τ_d, and the synchrotron frequency, ω_s. ß, the damping per synchrotron period is important in the transition from strong to weak instability. The coefficient in the square brackets is the approximated linear restoring force of the RF-potential with the collective force, F_c, from the interaction of the charge distribution with itself and its metallic surrounding. The induced voltage is obtained by the convolution of the longitudinal charge density with the wake function. The charge density, $\lambda(q,\tau)$, is given by $\lambda(q,\tau)=\int dp\,\psi(q,p,\tau)$. The wake function depends on the type of interaction studied. For this study we use the so called coherent synchrotron radiation, CSR-wake, shielded by parallel plates [4]. The details of the numerical solution of the VFP equation can be found in [5].

A similar approach was used by the Stanford group [2]. They found that for longer bunches and with strong instability the instability threshold can be described very well by a simple law relating the strength parameter, S_{csr}, with the shielding factor, Π: $S_{csr}=0.5+0.12\cdot\Pi$. Please see reference [2] for the definition of these scaling parameters or look at the captions at the axis in Fig. 1. These authors found that the instability is weak, meaning that the thresholds depend on β, if the bunch length, σ_z, is shorter than $0.85h^{3/2}/\rho^{1/2}$, with $2h$, the distance between the two shielding plates and ρ, the bending radius. The strong instability threshold is independent of the damping time, τ_d, and therefore does not depend on β.

Results of Simulations More systematic results of simulations for the transition regime are presented in Fig. 1. They were obtained with the code described in [5]. As can be seen, above a shielding factor $\Pi>\sim0.85$ the thresholds are only weakly dependent on β and the instability is strong. For shorter bunches thresholds depend on the damping. The half island of stability above the low lying threshold can be found for shielding values of Π within $0.65<\Pi<0.85$, however, only for $\beta<0.005$ corresponding to little damping per synchrotron period. Figure 2 shows the first mode of the instability in units of the zero current synchrotron frequency as a function of the shielding factor. For $\Pi>1$, and in the region of strong instability, this mode follows a simple law which relates it with the bunch length at the onset of the instability, σ_{inst}, and the resonance frequency created by the shielding plates [7], $F_{res}=c(\pi/3\rho)^{1/2}/d^{3/2}$: $F_{inst}/F_{syn}=2\pi\cdot F_{res}\cdot\sigma_{inst}$. With some ex-

* Work supported by the BMBF and the Land Berlin
[1] peter.kuske@helmholtz-berlin.de

ceptions, in the region of the weak instability it is mostly the quadrupole mode which shows up first.

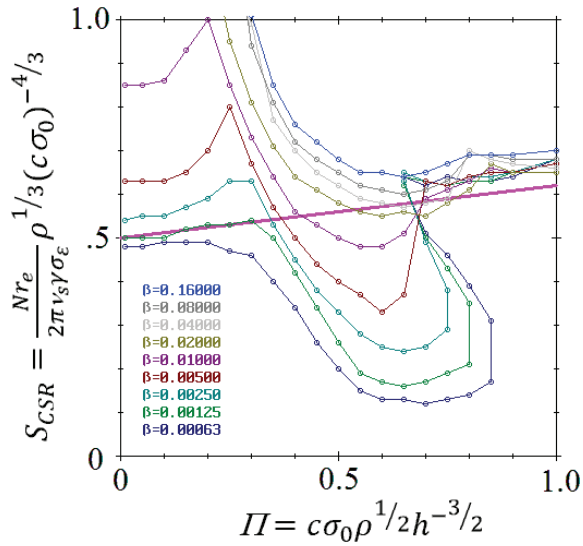

Figure 1: Threshold strength as a function of the shielding parameter for an increasing number of synchrotron periods per longitudinal damping time, i.e., from ~1 to ~256.

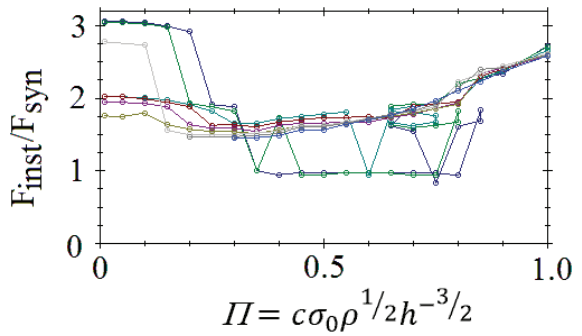

Figure 2: Mode number at the onset of instability as a function of the shielding factor for different β-factors (colours as in Fig. 1). For most cases the quadrupole mode shows up first. Exceptions are the low lying thresholds which is rather the dipole mode and for vanishing shielding, as Π goes to zero, the sextupole mode with very small values of β.

Simulation Results for the ANKA Experiments Figure 3 shows the theoretical thresholds in comparison to the experimental results [1]. The agreement is surprisingly good in view of the simplicity of the underlying theoretical model. There are however a few systematic differences which call for a more refined theory. For Π larger than 1 the measured thresholds are too low and the agreement with the simple scaling law is accidental. According to the simulations one would not expect to see the weak instability for Π-values in the range: $0.75 < \Pi < 0.85$ because the β is already too large in the experiment.

In Fig. 4 the comparison of the first unstable mode is shown. The general trend follows the predictions quite nicely which suggests that the resonance created by the shielding plates has the correct frequency. As already observed at BESSY II [6] and the CLS [8] the observed variation is clearly more step wise than the simple model predicts. This points to a smaller bandwidth of the resonator than given by the assumed circular motion of the electrons. One explanation could be the interference effect from neighbouring dipoles like in an optical klystron. This would lead to a smaller bandwidth of the resonance without changing its frequency.

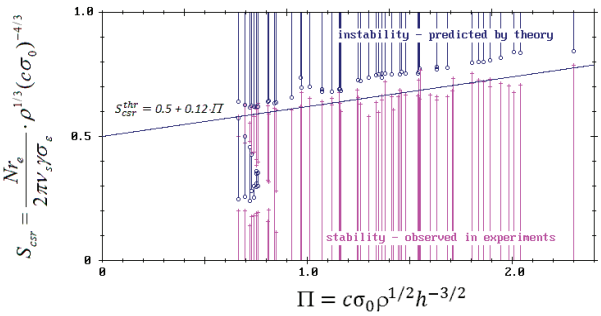

Figure 3: Comparison of experimental and theoretical results for the instability thresholds.

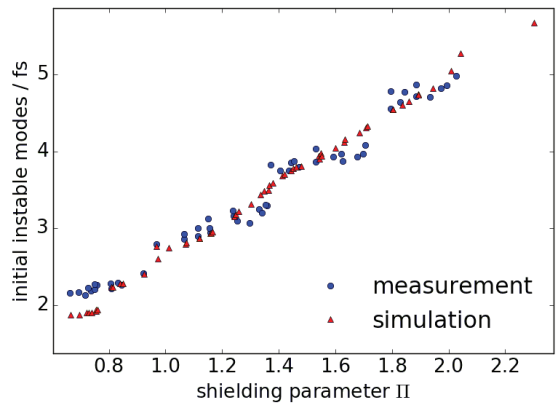

Figure 4: Comparison between measurement and simulation of the initial unstable mode as a function of the shielding factor (courtesy of M. Brosi).

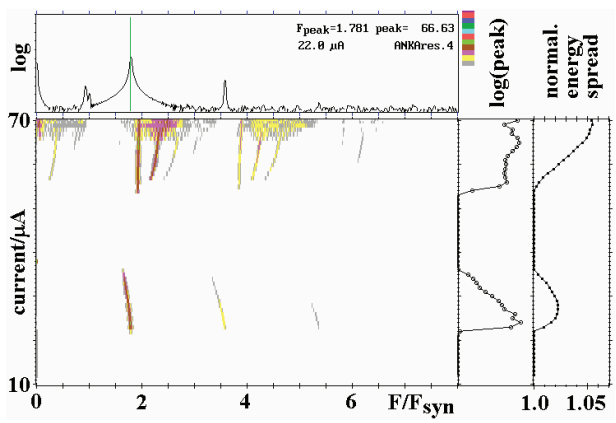

Figure 5: Waterfall display of simulated spectra as a function of the single bunch current (left). Peak values of individual spectra (middle) and normalised energy spread (right).

Figure 5 shows a typical spectrogram as produced from the simulated data. It agrees quite well with experimental

ISBN 978-3-95450-182-3

results [1]. The waterfall display of the spectra as a function of the bunch current is shown together with the peak value of the spectrum and the normalized energy spread. This demonstrates clearly that the onset of the instability and thus the increase of the energy spread can be extracted from the measured spectra obtained from the time dependent signals delivered by the μ-wave-detector.

EXTENSION OF THE THEORY

It was already mentioned that the pronounced stepwise increase of the mode numbers found in many experiments calls for a smaller resonance bandwidth as created by the simple circular motion of the electrons between two plates. This goes far beyond the intention of this paper. In the following the impact of the momentum dependence of the momentum compaction factor, α, is studied for a few selected cases.

Including Higher Order Terms in α

Higher order contributions to the momentum compaction factor, $\alpha=\alpha_0+\alpha_1\Delta p/p+\alpha_2(\Delta p/p)^2+...$, could be important for the calculation of the thresholds. This effect is included in the simulations in the following way: As explained in [5] the VFP-solver needs 4 steps per time step, $\Delta\tau$. In the first and third step the distribution function, g, has to be extrapolated after half a time step: $g_1=g_0(q-p\Delta\tau/2,p,\tau)$ where q, p, and $\Delta\tau$ are the dimensionless variables introduced at the beginning. Higher order terms are included through the following modification:
$q - p\,\Delta\tau/2 \rightarrow q - \left(p + \eta_1 p^2 + \eta_2 p^3 + \cdots\right)\Delta\tau/2$, with
$\eta_1 = (\alpha_1/a_0 - \alpha_0)\cdot\sigma_{\varepsilon_0}$, and
$\eta_2 = (\alpha_2/a_0 - 2\alpha_1 + \alpha_0)\cdot{\sigma_{\varepsilon_0}}^2$, where σ_{ε_0} is the natural relative energy spread. The VFP-solver was modified accordingly and checked against conceptually much simpler tracking calculations [9].

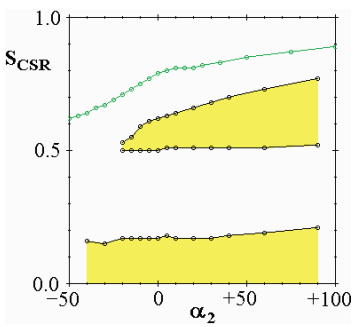

Figure 6: Thresholds in the region of the weak and strong instability as a function of α_2. With Π=0.7 bunches are stable in the yellow areas. In all cases α_1=0, α_0=3.23·10^{-4} for Π=0.7, and α_0=9.22·10^{-4} for Π=2.0 (shown in green).

Operating a storage ring with a small momentum compaction factor requires small α_1-terms in order to achieve a large momentum acceptance. The α_1-term usually is adjusted with the sextupole magnets to be close to zero. Octupole magnets are required for the control of the α_2-term. One of the few rings containing these multipole magnets is the MLS where they are routinely used to adjust the a_2-term between -20 and +14 with α_0~1.5·10^{-4} and α_1 close to zero [10] and these values have been verified experimentally by Compton back scattering. Thus the simulations were performed with the α_1-contribution set to zero and by changing only the α_2-term. The resulting thresholds as a function of α_2 are shown with β=0.00125 in Fig. 6 for the weak instability region of bunches at Π=0.7 and for the strong regime at Π=2.0. It is somewhat surprising that the thresholds of the weak instability depend very little on the α_2-term. It is rather the strong instability threshold which is influenced more strongly and with sufficiently large negative values the stable region above the low lying threshold disappears completely. Similar to the situation at Π=2 the simulation of the case at around Π=0.85, which showed the weak instability in the experiment, gave a shift to smaller upper (strong instability) thresholds for negative α_2 and α_2 as low as -20, however, the weak instability was not found.

CONCLUSION

Despite the simplicity of the parallel plate model the theoretical predictions are generally in surprisingly good agreement with many measurements. This is particularly true for the recent experimental results from ANKA where the discrepancies are quite small for the thresholds. Some of the deviations can be attributed to the too simple assumptions of an energy independent momentum compaction factor.

In many experiments pronounced steps in the initial instability mode were found when varying the bunch length. For comparison, simulations predict a more washed out dependency. This suggests that the resonance width or the corresponding Q-value are underestimated by the simple model of a circular orbit between two infinite and perfectly conducting plates. One possible modification could be to take into account the interaction of the radiation created in dipole magnets separated by a straight line and assuming a more or less smooth vacuum pipe.

These theoretical investigations are important for the funded BESSY VSR project which will produce very short bunches with a very high longitudinal voltage gradient. The shielding parameter becomes quite small (Π<0.4) and the synchrotron frequency will be high so that β<10^{-3}. There is not yet clear experimental evidence that for these parameters the thresholds will be given by the simple scaling law and that S_{csr} will approach 0.5 for the very short bunches achievable in the low-α optics mode.

ACKNOWLEDGEMENT

I thank Anke-Susanne Müller and her group at ANKA and especially Miriam Brosi for the close cooperation on this subject. She produced Figure 4 of this publication. I also would like to thank Andreas Jankowiak for his support.

REFERENCES

[1] M. Brosi, et al., Proceedings IPAC2016, Busan, Korea, TUPOR006, and to be published.

[2] K.L.F. Bane, *et al.*, Phys. Rev. ST-AB 13, 104402 (2010).

[3] M. Venturini, *et al.*, Phys. Rev. ST-AB 8, 014202 (2005).

[4] J. B. Murphy, *et al.*, Part. Accel. 57, 9 (1997).

[5] P. Kuske, "Calculation of longitudinal instability threshold currents for single bunches", Proceedings ICAP2012, Rostock- Warnemünde, Germany, THSDC3.

[6] P. Kuske, "CSR-driven longitudinal single bunch instability thresholds", Proceedings IPAC2013, Shanghai, China, WEOAB102.

[7] P. Kuske, "CSR-driven longitudinal instability - comparison of theoretical and experimental results", talk at the 3rd Low Emittance Ring Workshop, July, 2013, Oxford, UK.

[8] B.E. Billinghurst, *et al.*, PRAB 19, 020704 (2016).

[9] S.Y. Lee, "Accelerator Physics", 2nd edition, World Scientific Publishing Co. Pte. Ltd. (2004).

[10] M. Ries, PhD-thesis, `edoc.hu-berlin.de/dissertationen/ries-markus-2014-05-12/PDF/ries.pdf`, Humboldt-Universität zu Berlin, p52.

ISBN 978-3-95450-182-3